Biogeosciences Discuss., 6, 9127–9160, 2009
www.biogeosciences-discuss.net/6/9127/2009/

Biogeosciences Discussions

Biogeosciences Discussions is the access reviewed discussion forum of *Biogeosciences*

Evidence for greater oxygen decline rates in the coastal ocean than in the open ocean

D. Gilbert[1]**, N. N. Rabalais**[2]**, R. J. Diaz**[3]**, and J. Zhang**[4]

[1]Institut Maurice-Lamontagne, Pêches et Océans Canada, 850 Route de la mer, Mont-Joli, G5H 3Z4, Québec, Canada
[2]Louisiana Universities Marine Consortium, 8124 Highway 56, Chauvin, LA 70344, USA
[3]Virginia Institute of Marine Science, College of William and Mary, Gloucester Point, VA 23062, USA
[4]State Key Laboratory of Estuarine and Coastal Research, East China Normal University, 3663 Zhongshan Road North, Putuo District, Shanghai 200062, China

Received: 1 September 2009 – Accepted: 2 September 2009 – Published: 18 September 2009

Correspondence to: D. Gilbert (denis.gilbert@dfo-mpo.gc.ca)

Published by Copernicus Publications on behalf of the European Geosciences Union.

Abstract

In the global ocean, the number of reported hypoxic sites (oxygen <30% saturation) is on the rise both near the coast and in the open ocean. But unfortunately, most of the papers on hypoxia only present oxygen data from one or two years, so that we often lack a long-term perspective on whether oxygen levels at these locations are decreasing, steady or increasing. Consequently, we cannot rule out the possibility that many of the newly reported hypoxic areas were hypoxic in the past, and that the increasing number of hypoxic areas partly reflects increased research and monitoring efforts. Here we address this shortcoming by computing oxygen concentration trends in the global ocean from published time series and from time series that we calculated using a global oxygen database. Our results show that oxygen concentrations are generally decreasing in the ocean. They also reveal a greater percentage of negative trends for published oxygen time series than for oxygen time series computed from the global oxygen database, particularly in the open ocean. Finally, the oxygen decline rates computed from the global oxygen database are more severe in a 30 km band near the coast than in the open ocean, probably in response to human-caused eutrophication.

1 Introduction

Several studies suggest that oxygen levels are generally decreasing both in the coastal ocean (Diaz and Rosenberg, 2008) and in the deep ocean (Keeling and Garcia, 2002). This is cause for concern as lower concentrations of oxygen have adverse effects on marine life, ranging from reduced growth and reproductive capacity to habitat avoidance and ultimately death. At some coastal sites, eutrophication (Nixon, 1995) from nearby rivers appears to be the main cause of hypoxia (Kemp et al., 2005; Rabalais et al., 2002). But at other sites on the continental shelf and in the deep ocean, changes in ocean circulation (Gilbert et al., 2005; Monteiro et al., 2006) or in winter ventilation (Whitney et al., 2007) also play a role in lowering oxygen concentrations.

BGD

6, 9127–9160, 2009

To make things worse, biogeochemistry models embedded within ocean global circulation models (OGCM) generally predict that oxygen concentrations in the ocean will decrease in the coming decades as a consequence of global warming (Frölisher et al., 2009). There are early indications that this may already be detectable (Stramma et al., 2008; Johnson and Gruber, 2007), but interdecadal changes in ocean circulation could have played a role in these trends (Frölisher et al., 2009).

According to Diaz and Rosenberg (2008), the number of hypoxic sites around the world reported in the scientific literature has increased about an order of magnitude (40 to 400 sites) from the 1960s to the present. This seems to indicate that hypoxia is becoming much more widespread and more severe relative to the historical literature. But we need to be careful in order to interpret this finding correctly. The fact that more papers dealing with coastal hypoxia started to appear since the 1990s could also indicate that scientists have devoted more efforts to detecting and reporting hypoxia. Do the new reports of hypoxic conditions reflect a truly widespread phenomenon, or do they reflect a greater tendency for scientists to report low oxygen conditions, because of the associated adverse ecological implications, than to report stable or increasing oxygen levels?

In this paper, we compile global oxygen trend statistics from a coastal band (0 to 30 km from shoreline), from a transition band (30 to 100 km from shoreline) and from the open ocean (>100 km from shoreline). In each distance category, the mean trends, median trends and percentage of negative trends are calculated from oxygen time series published in refereed journals, and from oxygen time series obtained from a global oxygen database. In Sect. 2, we provide the details of our search for papers containing plots of oxygen time series spanning at least one decade, and how we determined trends from these time series. We also describe the methods used to merge various public databases in order to construct oxygen timeseries at fixed stations and compute trends from them. In Sect. 3, we present maps, a histogram, and statistics of oxygen trends based on the scientific literature, and based on our analyses from the raw data at fixed stations in the global ocean. In Sect. 4, we discuss the implications of our findings, and we present the main conclusions in Sect. 5.

2 Materials and methods

2.1 Published oxygen time series

Because decadal oxygen variability is important in most marine systems (Garcia et al., 2005), we required that oxygen time series have a duration of at least 10 years. This selection criterion allows us to remove some of the unwanted noise associated with interannual to decadal variability. Being concerned with the large diurnal oxygen cycles that are characteristic of shallow estuaries (e.g., Tyler et al., 2009), we also limited our attention to sites where the bottom was at least 10 m deep, because timing of sampling will influence the oxygen reading and complicate the analyses in these shallower systems. Finally, we restricted our attention to oxygen time series consisting of chemical titration methods only (e.g. Winkler, 1888; Carpenter, 1965; Grasshoff et al., 1999), thus excluding data from electronic oxygen sensors from our analyses. We realize this severely hampers data availability, as more and more people use polarographic or optical sensors to measure oxygen. These oxygen probes can provide excellent data when they are routinely calibrated against Winkler titrations. But in many laboratories, the lack of regular sensor calibration can lead to inaccurate or suspicious data. The National Oceanographic Data Center (NODC) took the decision to only use oxygen data believed to be obtained by chemical titration methods in their production of the climatological World Ocean Atlas 2005 (Garcia et al., 2006), and we followed their example by erring on the side of caution for this global ocean data analysis. With respect to the calculation of trends, only using Winkler titrations offers an additional benefit. It avoids the possibility of introducing artificial jumps in the time series arising from a change in measurement method.

We restricted our literature search with the ASFA (Aquatic Sciences and Fisheries Abstracts) and SCOPUS bibliography databases to papers with publication dates of

1985 and later. Some time series were eliminated from our analyses because they did not contain precise depth information (e.g. Lysiak-Pastuszak et al., 2004) for their measurements. In other cases, the individual data points were so cluttered that digitization was virtually impossible to do in a reliable way. One such cluttered time series, from Justić et al. (1987), was nevertheless included in our study by using their trend estimate for the bottom waters of the northern Adriatic Sea and converting the original concentration units of $cm^3 dm^{-3}$ to $\mu mol L^{-1}$ (Table 1). Other oxygen time series with original concentration units other than $\mu mol L^{-1}$ were also converted using the factors given in Table 1.

For refereed journal papers in which near-bottom oxygen values were plotted, it was sometimes necessary to make an educated guess about the depth of the time series based on local bathymetry (Conley et al., 2007; Peng et al., 2009). In other cases, we had to estimate the climatological depth of isopycnal surfaces (Kang et al., 2004; Konovalov and Murray, 2001; Nakanowatari et al., 2007). In one instance (Lin et al., 2005), we had to correct the originally published oxygen time series (with concentrations over 600 $\mu mol L^{-1}$) by dividing the published concentrations by a factor of two. The origin of this error in data reporting remains unclear, but one possibility is that the authors reported atomic (O) rather than molecular (O2) DO concentrations.

Figure 1 shows the locations of the published oxygen time series used in our study. The regions of the Kattegat, Baltic Sea and Black Sea represent our most abundant sources of published oxygen data. Other areas with reasonable geographic coverage include the East/Japan Sea and coastal waters around Japan and North America. Unfortunately, a single time series from the southern hemisphere satisfied our selection criteria (Monteiro et al., 2008). A subsample of digitized oxygen time series is plotted on Fig. 2. In some cases, negative oxygen values indicate the presence of H_2S which represents an oxygen debt and was converted to oxygen concentration after multiplying the H_2S concentration by −2. In fact, the four deepest oxygen time series from Konovalov and Murray (2001) listed in Table 2 are actually H_2S time series. We determined oxygen trends over the entire length of the published oxygen time series by simple linear regression.

2.2 Oxygen time series from a global dataset

Most of the oxygen data used in this paper come from a series of queries made in September 2008 at the National Oceanographic Data Center (NODC) of the United States. While the NODC database is global in scope, it is never entirely up-to-date, often missing substantial data from the most recent years. Our second most important source of oxygen data is the ICES (International Council for the Exploration of the Sea) database, from which we also ran a series of queries in September 2008. To this, we added two Canadian databases: the national Biochem database from ISDM (Integrated Science Data Management, Dept. of Fisheries and Oceans, Ottawa, Ontario, Canada) and a northeast Pacific and Arctic database held at the Institute of Ocean Sciences (Sidney, BC, Canada). Finally, we also obtained oxygen data from the CARIACO (Carbon Retention In A Colored Ocean) Project database (e.g. Müller-Karger et al., 2001). Since a significant proportion of the above oxygen data can be present in more than one database, we had to eliminate all duplicate records based on metadata information on the latitude, longitude, date and time (UTC) of the measurements.

Based on prior knowledge of long-term ocean monitoring programs, and on visual inspection of plots of oxygen data distribution in space and time, we selected 2132 fixed stations (Fig. 3) for the calculation of oxygen time series from raw oxygen data. For each "fixed" station, we determined the latitude and longitude coordinates of the center and allowed a data search radius of 10 km. Then for each year, we calculated mean oxygen values at the depths of 0 m (0–2 m), 10±1 m, 20±2.5 m, 50±5 m, 75±5 m, 100±5 m, 150± 10 m, 200±10 m, 250±10 m and 300±10 m. To avoid variability in the oxygen time series associated with seasonal cycles, our analyses were limited to the summer months of July, August and September from the sea surface to 75 m depth. At depths of 100 m and greater, where the seasonal cycles are much weaker, we used all available oxygen data from the twelve months of the year. Combining the trend estimates at 0, 50, 100, 150, 200, 250 and 300 m, we also calculated oxygen trend statistics for the 0 to 300 m depth range.

For the calculation of oxygen trends in a standard reference period (e.g. 1951–2000), we imposed a criterion of 30% overall data availability, and requested at least one year with data in both halves of the time series. For example, for 25-year reference periods, we required at least 8 years with oxygen data. In addition, for the 1951–1975 period, we required at least one year with data before and after the middle year of 1973. Similarly, for the 1976–2000 period, we required at least one year with data before and after the middle year of 1988. At some stations, oxygen concentrations can be very close to or equal to zero at certain depths over most of the 25-year period under consideration. In such cases, unless there is accompanying H_2S data that can be converted to negative oxygen concentrations, the oxygen trend could be meaningless. There exist some locations where H_2S data have been collected over many years (e.g. Fonselius and Valderrama, 2003; Konovalov and Murray, 2001), but this is not always the case. To ensure uniformity in our results, we therefore decided to eliminate time series where the median oxygen concentration was less than 10 μmol L^{-1}. Locations affected by this decision include the deep basins of the Baltic Sea, central Black Sea, Saanich Inlet, Cariaco Basin, and stations located in oxygen minimum zones off Peru, Chile, and India (Fig. 4).

2.3 Grouping of trends based on distance from the coast

Due to the effect of Earth's rotation, river plumes generally veer to the right (left) of river mouths in the Northern (Southern) Hemisphere, and then tend to flow parallel to the coastline within about one internal Rossby radius of deformation (Gill, 1982). We take 30 km as a representative value of one internal Rossby radius of deformation between 20° and 60° of latitude (Chelton et al., 1998). Based on ocean physics, we expect that most of the impacts of human-induced eutrophication should be felt within this coastal band of 30 km width; albeit, there are exceptions such as the Gulf of Mexico hypoxic zone associated with the Mississippi River plume that extends farther offshore (Rabalais et al., 2007).

Of course, the internal Rossby radius of deformation varies with seasonal stratification strength, but it depends mostly on latitude, with typical values of roughly 10 km at 60°, 20 km at 45°, 40 km at 30° and 80 km at 15° (Chelton et al., 1998). Given these values, we arbitrarily take 100 km as a representative distance beyond which a parcel of water is no longer under the direct influence of nutrient-rich, buoyant river plumes and coastal currents. We shall refer to this distance category (>100 km from the coast) as the open ocean. Finally, between the coastal band (0–30 km) and the open ocean, we define a transition zone with distances from the shoreline between 30 km and 100 km.

We evaluated distance from the coast for each station by using GSHHS (Global Self-consistent, Hierarchical, High-resolution Shoreline) shapefiles version 1.3 (Wessel and Smith, 1996), together with the functions distance m and deg2 km m from the Matlab mapping toolbox version 2.7.2. The GSHHS shoreline exists in five spatial resolutions (crude, low, intermediate, high and full). We used the intermediate spatial resolution, which allowed us to determine distance from a fixed station to the shoreline with an estimated accuracy of about 1 km at a reasonable computing cost.

3 Results

3.1 Published time series

Table 2 gives the linear trend of each published oxygen timeseries, together with its latitude, longitude, depth, time period over which the trend was estimated, distance from the coast, and journal reference. An overall summary of these trends based on distance from the coast is given in Table 3. In the 0–30 km coastal band, we find a median oxygen trend of $-0.98\,\mu\mathrm{mol\,L^{-1}yr^{-1}}$. The median oxygen trends in the other two distance bands are also negative, but less so than in the coastal band. The story is different for the mean published oxygen trends. The most negative mean trend value ($-0.74\pm0.44\,\mu\mathrm{mol\,L^{-1}yr^{-1}}$) is from the open ocean, with mean values that are not different from zero in the other two distance bands. If we consider all categories of distance from the coast at once, the mean of all published oxygen trends ($-0.36\pm0.52\,\mu$mol $L^{-1}yr^{-1}$) is negative, although not significantly different from zero (Table 3, Fig. 5) at the 95% confidence level. The overall median published oxygen trend is $-0.62\,\mu$mol $L^{-1}yr^{-1}$, with 73% of all published oxygen time series displaying negative trends. A global map of oxygen trends determined from published time series is shown in Fig. 6. To interpret this map correctly, it is necessary to consider that at certain fixed stations (e.g. station P in Whitney et al., 2007), we have trend estimates from more than one depth level and these are overlain on top of each other. This map shows the general prevalence of negative published oxygen trends, but also highlights a great deal of variability in trend estimates.

3.2 Calculated time series

In the 0–30 km coastal band, the mean oxygen trend is negative (at the 95% confidence level) at seven of the ten standard depths, but is not statistically different from zero at the three remaining depths (Table 4). The percentage of oxygen time series with negative trends is greater than 50% at eight of the 10 depths, and the median trend is negative at nine of the ten depths. The number of time series from stations located near small islands are indicated in Table 4 because we do not expect these oxygen time series to be as much influenced by human activities compared with stations located near continents. Impacts of dissolved and particulate nutrients on coastal ecosystems depend on how efficiently these nutrients are retained in nearshore areas. And clearly, the degree of retainment will be higher in coastal embayments than around a small island subjected to time varying open ocean currents and eddies. The mean oxygen trend over the 0 to 300 m depth range is $-0.35\,\mu$mol $L^{-1}yr^{-1}$ (between -0.47 and $-0.24\,\mu$mol $L^{-1}yr^{-1}$ at the 95% confidence level).

In the 30–100 km transition band between the coastal zone and the open ocean, the mean oxygen trend is negative at six of the ten standard depths, is not statistically different from zero at three depths, and is positive at 75 m depth (Table 5). The percentage of oxygen time series with negative trends is greater than 50% at all depths but 75 m. Likewise, the median trend is negative at all depths but 75 m. The mean oxygen trend over the 0 to 300 m depth range is -0.19 μmol L^{-1}yr^{-1} (between −0.27 and −0.10 μmol L^{-1}yr^{-1} at the 95% confidence level).

Finally, for open ocean stations located at distances greater than 100 km from the shoreline, the mean oxygen trend is negative at four of the ten standard depths, but is not statistically different from zero at the six other depths (Table 6). The percentage of oxygen time series with negative trends is greater than 50% at six of the ten depths, and the median trend is negative at the same six depths out of ten. The mean oxygen trend over the 0 to 300 m depth range is −0.09 μmol L^{-1}yr^{-1} (between −0.15 and −0.03 μmol L^{-1}yr^{-1} at the 95% confidence level).

Regardless of the distance from coast category, the coefficient of variation (standard deviation/mean) is generally much larger than one. Thus, many time series are required in order to estimate the overall mean trend to within a certain level of accuracy (Hakanson and Stenstrom-Khalili, 2009).

Oxygen trend estimates display greater variability over short reference periods (e.g. 1991–2000) than over longer reference periods (e.g. 1951–2000), as can be seen from the colorbar scales of trends for waters surrounding Japan (Fig. 7) and Europe (Fig. 8). Comparing oxygen trend estimates from the 25-year periods 1951–1975 and 1976–2000 in Figs. 7 and 8, we see qualitative evidence for a greater proportion of negative trends in the 1976–2000 period than in the 1951–1975 period, which we tested statistically. Changes in the estimated trends in DO, either positive or negative, were compared between the two 25-year periods (1951–1975 and 1976–2000) using logistic regression. Data were also categorized into depth intervals (lower limits of each category being 0, 10, 20, 50, 75, 100, 150, 200, 250, 300 m) and distance from the coastline (<30, 30–100, and >100 km). There was no multicolinearity between depth and distance from coastline (variance inflation was 1.00 for both variables). This was assessed using a weighted least squares regression of the predicted probabilities from the logistic regression. These statistical analyses were performed using SAS. Overall, increasing depth lowered the odds of a negative trend as did increasing distance from the coastline. But the time period had the largest effect on DO trends. Between 1951–1975 and 1976–2000 the odds of a negative DO trend occurring increased by over a factor of 2 ($p<0.001$). Collectively, these findings are consistent with greater prevalence of coastal hypoxia in more recent years.

4 Discussion

The median published trends given in Table 3 for the 0–30 km band (−0.98 μmol L^{-1}yr^{-1}), the 30–100 km band (−0.88 μmol L^{-1}yr^{-1}), and the 100 km+ band (−0.54 μmol L^{-1}yr^{-1}), are more negative than the median trends for any single depth in Tables 4, 5 and 6 respectively. This suggests that in general, scientists have a greater tendency to publish papers containing oxygen time series plots when the trend is strongly negative than when the trend is either neutral or positive. This tendency to preferentially report negative oxygen trends appears to be more pronounced in the open ocean than in the coastal ocean. Indeed, for the coastal ocean, the percentage of published negative oxygen trends (70.7%, between 54.5% and 83.9% at the 95% confidence level), is very similar to the percentages of negative trends computed from the raw data of the global oxygen database (Tables 3 and 4). On the other hand, in the open ocean, the percentage of published negative oxygen trends (77.5%, between 61.5% and 89.2% at the 95% confidence level), is higher than nine of the ten percentages of negative trends computed from the raw data of the global oxygen database (Tables 3 and 6).

A number of biogeochemical models embedded within ocean circulation models (Sarmiento et al., 1998; Matear et al., 2000; Bopp et al., 2002) predicted that as a consequence of global warming, oxygen levels in the ocean will decrease at a rate that is typically three to four times faster than one might expect based on changes in oxygen solubility alone (Garcia and Gordon, 1992). For instance, Frölisher et al. (2009) predicted oxygen concentration trends of −0.04 to −0.07 μmol L^{-1}yr^{-1} from 1990–1999 to 2090–2099 in the upper 300 m of the Atlantic and Pacific Oceans.

These modelled trend values are not inconsistent with the mean trend value of $-0.09\pm0.06\,\mu\text{mol}\,\text{L}^{-1}\text{yr}^{-1}$ obtained in this study for the open ocean (Table 6). However, detailed comparisons between our results and biogeochemical model predictions cannot be made with confidence due to the poor spatial coverage of the global ocean afforded by our limited set of fixed stations (Fig. 3).

Our results are affected by substantial decadal oxygen variability (Garcia et al., 2005) caused by large scale changes in atmospheric and oceanic circulation patterns associated with the El Niño Southern Oscillation (McPhaden et al., 2006), the North Atlantic Oscillation (Hurrell and Deser, 2009) and the Pacific Decadal Oscillation (Mantua and Hare, 2002) for example. The importance of decadal variability is depicted for a few individual time series on Fig. 2, and is largely responsible for the very different patterns of oxygen trends obtained for different reference periods (Figs. 7 and 8).

5 Conclusions

In this paper, we have shown that

- The median published oxygen trends are more negative than the median trends computed from raw oxygen data, suggesting a publication bias in favor of strongly negative trends that is likely due to the adverse ecosystem implications of hypoxia.
- Based on the raw data analysis, oxygen trends in the 1976–2000 period are more negative than in the 1951–1975 period, indicating a recent worsening of hypoxia.
- Based on the raw data analysis for the 1976–2000 period, oxygen concentrations are declining faster in the coastal ocean ($-0.35\pm0.12\,\mu\text{mol}\,\text{L}^{-1}\text{yr}^{-1}$) than in the open ocean ($-0.09\pm0.06\,\mu\text{mol}\,\text{L}^{-1}\text{yr}^{-1}$) between 0 and 300 m depth.

Acknowledgements. We thank Guillaume Hardy who imported oxygen data from the public databases into Matlab and wrote programs for statistical analysis and mapping. Benoît Roberge and Audrey Guérard digitized the oxygen time series from refereed journal publications. We are indebted to the thousands of scientists who made oxygen measurements and sent their data to national and international data archive centers. This research was funded by the Climate Change Science Initiative of the Department of Fisheries and Oceans Canada, and was initiated as part of the activities of SCOR (Scientific Committee on Oceanic Research) Working Group 128 on "Natural and human-induced hypoxia and consequences for coastal areas".

References

Aure, J. and Dahl, E.: Oxygen, nutrients, carbon and water exchange in the Skagerrak Basin, Cont. Shelf Res., 14, 965–977, 1994. 9146

Blindheim, J. and Rey, F.: Water-mass formation and distribution in the Nordic Seas during the 1990s, ICES J. Mar. Sci., 61, 846–863, 2004. 9146

Bograd, S. J., Castro, C. G., Di Lorenzo, E., Palacios, D. M., Bailey, H., Gilly, W., and Chavez, F. P.: Oxygen declines and the shoaling of the hypoxic boundary in the California Current, Geophys. Res. Lett., 35, L12607, doi:10.1029/2008GL034185, 2008. 9146

Bopp, L., Le Quéré, C., Heimann, M., Manning, A. C., and Monfray, P.: Climate-induced oceanic oxygen fluxes: Implications for the contemporary carbon budget, Global Biogeochem. Cy., 16, 6–1, 2002. 9137

Carpenter, J. H.: The Chesapeake Bay Institute technique for the Winkler dissolved oxygen method, Limnol. Oceanogr., 10, 141–143, 1965. 9130

Chelton, D. B., Deszoeke, R. A., Schlax, M. G., El Naggar, K., and Siwertz, N.: Geographical variability of the first baroclinic Rossby radius of deformation, J. Phys. Oceanogr., 28, 433–460, 1998. 9133, 9134

Conley, D. J., Carstensen, J., AErtebjerg, G., Christensen, P. B., Dalsgaard, T., Hansen, J. L. S., and Josefson, A. B.: Long-term changes and impacts of hypoxia in Danish coastal waters, Ecol. Appl., 17, S165–S184, 2007. 9131, 9146

Cronin, T. M. and Vann, C. D.: The sedimentary record of climatic and anthropogenic influence on the Patuxent estuary and Chesapeake Bay ecosystems, Estuaries, 26, 196–209, 2003. 9146

Diaz, R. and Rosenberg, R.: Spreading dead zones and consequences for marine ecosystems, Science, 321, 926–929, doi:10.1126/science.1156401, 2008. 9128, 9129

Fonselius, S. and Valderrama, J.: One hundred years of hydrographic measurements in the Baltic Sea, J. Sea Res., 49, 229–241, doi:10.1016/S1385-1101(03)00035-2, 2003. 9133, 9146

Frölisher, T., Joos, F., Plattner, G.-K., Steinacher, M., and Doney, S. C.: Natural variability and anthropogenic trends in oceanic oxygen in a coupled carbon cycle-climate model ensemble, Global Biogeochem. Cy, 23, GB1003, doi:10.1029/2008GB003316, 2009. 9129, 9137

Garcia, H. E. and Gordon, L. I.: Oxygen solubility in seawater: Better fitting equations, Limnol. Oceanogr., 37, 1307–1312, 1992. 9137

Garcia, H. E., Boyer, T. P., Levitus, S., Locarnini, R. A., and Antonov, J.: On the variability of dissolved oxygen and apparent oxygen utilization content for the upper world ocean: 1955 to 1998, Geophys. Res. Lett., 32, L09604, doi:10.1029/2004GL022286, 2005. 9130, 9138

Garcia, H. E., Locarnini, R. A., Boyer, T. P., and Antonov, J. I.: World Ocean Atlas 2005: Dissolved oxygen, apparent oxygen utilization, and oxygen saturation, Vol. 3 of *NOAA Atlas NESDIS 63*, US Government Printing Office, Washington, DC, 2006. 9130

Gilbert, D., Sundby, B., Gobeil, C., Mucci, A., and Tremblay, G.-H.: A seventy-two-year record of diminishing deep-water oxygen in the St. Lawrence estuary: The northwest Atlantic connection, Limnol. Oceanogr., 50, 1654–1666, 2005. 9128, 9146

Gill, A. E.: Atmosphere-ocean dynamics, vol. 30 of *International geophysics series*, Academic Press, New York, USA, 1982. 9133

Grasshoff, K., Kremling, K., and Ehrhardt, M.: Methods of seawater analysis, Wiley-VCH, Toronto, Canada, 3rd edn., 1999. 9130

Hakanson, L. and Stenstrom-Khalili, M. I.: Uncertainties in data and spurious correlations related to the Redfield ratio, Int. Rev. Hydrobiol., 94, 338–351, doi:10.1002/iroh.200811110, 2009. 9136

Hurrell, J. W. and Deser, C.: North Atlantic climate variability: The role of the North Atlantic Oscillation, J. Marine Syst., 78, 28–41, doi:10.1016/j.jmarsys.2008.11.026, 2009. 9138

Johnson, G. C. and Gruber, N.: Decadal water mass variations along 20° W in the northeastern Atlantic Ocean, Prog. Oceanogr., 73, 277–295, 2007. 9129

Justić, D., Legović, T., and Rottini-Sandrini, L.: Trends in oxygen content 1911–1984 and occurrence of benthic mortality in the northern Adriatic Sea, Estuar. Coast. Shelf S., 25, 435–445, 1987. 9131, 9146

Kang, D., Kim, J., Lee, T., and Kim, K.: Will the East/Japan Sea become an anoxic sea in the next century?, Mar. Chem., 91, 77–84, 2004. 9131, 9146

Kasai, A., Yamada, T., and Takeda, H.: Flow structure and hypoxia in Hiuchi-nada, Seto Inland Sea, Japan, Estuar. Coast. Shelf S., 71, 210–217, 2007. 9146

Keeling, R. F. and Garcia, H. E.: The change in oceanic O2 inventory associated with recent global warming, Proc. Nat. Acad. Sci., 99(12), 7848-7853, 2002. 9128

Kemp, W. M., Boynton, W. R., Adolf, J. E., Boesch, D. F., Boicourt, W. C., Brush, G., Cornwell, J. C., Fisher, T. R., Glibert, P. M., Hagy, J. D., Harding, L. W., Houde, E. D., Kimmel, D. G., Miller, W. D., Newell, R. I. E., Roman, M. R., Smith, E. M., and Stevenson, J. C.: Eutrophication of Chesapeake Bay: historical trends and ecological interactions, Mar. Ecol. Prog. Ser., 303, 1–29, doi:10.3354/meps303001, 2005. 9128

Konovalov, S. K. and Murray, J. W.: Variations in the chemistry of the Black Sea on a time scale of decades (1960–1995), J. Marine Syst., 31, 217–243, 2001. 9131, 9133, 9146

Laine, A. O., Sandler, H., Andersin, A. ., and Stigzelius, J.: Long-term changes of macrozoobenthos in the Eastern Gotland Basin and the Gulf of Finland (Baltic Sea) in relation to the hydrographical regime, J. Sea Res., 38, 135–159, 1997. 9147, 9149

Laine, A. O., Andersin, A. ., Leinio, S., and Zuur, A. F.: Stratification-induced hypoxia as a structuring factor of macrozoobenthos in the open Gulf of Finland (Baltic Sea), J. Sea Res., 57, 65–77, 2007. 9147

Lin, C., Ning, X., Su, J., Lin, Y., and Xu, B.: Environmental changes and the responses of the ecosystems of the Yellow Sea during 1976–2000, J. Marine Syst., 55, 223–234, 2005. 9131, 9147

Lysiak-Pastuszak, E., Drgas, N., and Piatkowska, Z.: Eutrophication in the Polish coastal zone: The past, present status and future scenarios, Mar. Pollut. Bull., 49, 186–195, doi:10.1016/j.marpolbul.2004.02.007, 2004. 9131

Mantua, N. J. and Hare, S. R.: The Pacific Decadal Oscillation, J. Oceanogr., 58, 35–44, 2002. 9138

Matear, R. J., Hirst, A. C., and McNeil, B. I.: Changes in dissolved oxygen in the Southern Ocean with climate change, Geochem. Geophy. Geosy., 1, Geochem. Geophy. Geosy., 1, Paper number 2000GC000086, 2000. 9137

McPhaden, M. J., Zebiak, S. E., and Glantz, M. H.: ENSO as an integrating concept in earth science, Science, 314, 1740–1745, doi:10.1126/science.1132588, 2006. 9138

Minami, H., Kano, Y., and Ocawa, K.: Long-term variations of potential temperature and dis-

solved oxygen of the Japan Sea Proper Water, J. Oceanogr., 55, 197–205, 1999. 9147
Monteiro, P. M. S., Van Der Plas, A., Mohrholz, V., Mabille, E., Pascall, A., and Joubert, W.: Variability of natural hypoxia and methane in a coastal upwelling system: Oceanic physics or shelf biology?, Geophys. Res. Lett., 33, doi:10.1029/2006GL026234, 2006. 9128
Monteiro, P. M. S., van der Plas, A. K., Mélice, J.-L., and Florenchie, P.: Interannual hypoxia variability in a coastal upwelling system: Ocean-shelf exchange, climate and ecosystem-state implications, Deep-Sea Res. Pt I, 55, 435–450, doi:10.1016/j.dsr.2007.12.010, 2008. 9131, 9147
Müller-Karger, F., Varela, R., Thunell, R., Scranton, M., Bohrer, R., Taylor, G., Capelo, J., Astor, Y., Tappa, E., Ho, T. ., and Walsh, J. J.: Annual cycle of primary production in the Cariaco Basin: Response to upwelling and implications for vertical export, J. Geophys. Res.-Oceans, 106, 4527–4542, 2001. 9132
Nakanowatari, T., Ohshima, K. I., and Wakatsuchi, M.: Warming and oxygen decrease of intermediate water in the northwestern North Pacific, originating from the Sea of Okhotsk, 1955–2004, Geophys. Res. Lett., 34, 2007. 9131, 9147
Nixon, S. W.: Coastal marine eutrophication: a definition, social causes and future concerns, Ophelia, 41, 199–219, 1995. 9128
Nordberg, K., Gustafsson, M., and Krantz, A.: Decreasing oxygen concentrations in the Gullmar Fjord, Sweden, as confirmed by benthic foraminifera, and the possible association with NAO, J. Marine Syst., 23, 303–316, 2000. 9147
Peng, S., Dai, M., Hu, Y., Bai, Z., and Zhou, R.: Long-term (1996–2006) variation of nitrogen and phosphorus and their spatial distributions in Tianjin coastal seawater, B. Envir. Contam. Tox., 83, 416–421, doi:10.1007/s00128-009-9680-1, 2009. 9131, 9147
Petrie, B. and Yeats, P.: Annual and interannual variability of nutrients and their estimated fluxes in the Scotian Shelf – Gulf of Maine region, Can. J. Fish. Aquat. Sci., 57, 2536–2546, 2000. 9148
Pitkänen, H., Lehtoranta, J., and Räike, A.: Internal nutrient fluxes counteract decreases in external load: The case of the estuarial eastern Gulf of Finland, Baltic Sea, Ambio, 30, 195–201, 2001. 9148
Pohl, C. and Hennings, U.: The coupling of long-term trace metal trends to internal trace metal fluxes at the oxic-anoxic interface in the Gotland Basin (5719,20 N; 2003,00 E) Baltic Sea, J. Marine Syst., 56, 207–225, doi:10.1016/j.jmarsys.2004.10.001, 2005. 9148
Rabalais, N. N., Turner, R. E., and Wiseman Jr., W. J.: Gulf of Mexico hypoxia, a.k.a. “The dead

zone", Ann. Rev. Ecol. Syst., 33, 235–263, doi:10.1146/annurev.ecolsys.33.010802.150513, 2002. 9128

Rabalais, N. N., Turner, R. E., Sen Gupta, B. K., Boesch, D. F., Chapman, P., and Murrell, M. C.: Hypoxia in the northern Gulf of Mexico: Does the science support the plan to reduce, mitigate, and control hypoxia?, Estuaries Coasts, 30, 753–772, 2007. 9133

Rosenberg, R.: Negative oxygen trends in Swedish coastal bottom waters, Mar. Pollut. Bull., 21, 335–339, 1990. 9148

Sarmiento, J. L., Hughes, T. M. C., Stouffer, R. J., and Manabe, S.: Simulated response of the ocean carbon cycle to anthropogenic climate warming, Nature, 393, 245–249, 1998. 9137

Stramma, L., Johnson, G. C., Sprintall, J., and Mohrholz, V.: Expanding oxygen-minimum zones in the tropical oceans, Science, 320, 655–658, doi:10.1126/science.1153847, 2008. 9129

Swanson, R. L. and Parker, C. A.: Physical environmental factors contributing to recurring hypoxia in the New York Bight, Trans. Am. Fish. Soc., 117, 37–47, 1988. 9148

Turner, R. E., Rabalais, N. N., Swenson, E. M., Kasprzak, M., and Romaire, T.: Summer hypoxia in the northern Gulf of Mexico and its prediction from 1978 to 1995, Mar. Environ. Res., 59, 65–77, 2005. 9148

Tyler, R. M., Brady, D. C., and Targett, T. E.: Temporal and spatial dynamics of diel-cycling hypoxia in estuarine tributaries, Estuaries Coasts, 32, 123–145, doi:10.1007/s12237-008-9108-x, 2009. 9130

Weichart, G., Heise, G., and Becker, G. A.: A new concept for the assessment of the oxygen situation in a shelf sea area, Dt. Hydrogr. Z., 46, 263–275, 1994. 9148

Wessel, P. and Smith, W. H. F.: A Global Self-consistent, Hierarchical, High-resolution Shoreline database, J. Geophys. Res.-Sol. Ea., 101, 8741–8743, 1996. 9134

Whitney, F. A., Freeland, H. J., and Robert, M.: Persistently declining oxygen levels in the interior waters of the eastern subarctic Pacific, Prog. Oceanogr., 75, 179–199, 2007. 9128, 9135, 9148

Wilson, R. E., Swanson, R. L., and Crowley, H. A.: Perspectives on long-term variations in hypoxic conditions in western Long Island Sound, J. Geophys. Res.-Oceans, 113, C12011, doi:10.1029/2007JC004693, 2008. 9148

Winkler, L.: Die Bestimmung des im Wasser gelsten Sauerstoffen, Ber. Dtsche. Chem. Ges., 21, 2843–2855, 1888. 9130

Yakushev, E. V., Chasovnikov, V. K., Debolskaya, E. I., Egorov, A. V., Makkaveev, P. N., Pakhomova, S. V., Podymov, O. I., and Yakubenko, V. G.: The northeastern Black Sea redox zone: Hydrochemical structure and its temporal variability, Deep-Sea Res. Pt II, 53, 1769–1786, 2006. 9148

Yasuhara, M., Yamazaki, H., Tsujimoto, A., and Hirose, K.: The effect of long-term spatiotemporal variations in urbanization-induced eutrophication on a benthic ecosystem, Osaka Bay, Japan, Limnol. Oceanogr., 52, 1633–1644, 2007. 9148

Yunev, O. A., Carstensen, J., Moncheva, S., Khaliulin, A., Aertebjerg, G., and Nixon, S.: Nutrient and phytoplankton trends on the western Black Sea shelf in response to cultural eutrophication and climate changes, Estuar. Coast. Shelf S., 74, 63–76, 2007. 9148

BGD
6, 9127–9160, 2009

Oxygen trends in the ocean

D. Gilbert et al.

Table 1. Conversion factors to transform oxygen concentrations from the original reported units to μmol L^{-1}.

Original units	Conversion factor
mg L^{-1}	31.231
mL L^{-1}	46.615
cm^3 dm^{-3}	46.615
mg atom m^{-3}	1
μmol kg^{-1}	$\sim$1

Table 2. List of refereed journal publications from which we obtained oxygen trends, or digitized oxygen time series and then calculated the trends. Oxygen trends are given in $\mu mol\,L^{-1} yr^{-1}$ and the distances are relative to the nearest shoreline from a continent or island.

Marine System	Latitude, Longitude	Depth (m)	Time period	Trend	Distance (km)	Reference
Skagerrak Basin	58.22, 9.50	600	1953–1991	−0.11	45	Aure and Dahl (1994)
Greenland Basin	74.75, −0.50	2500	1981–2000	−0.83	467	Blindheim and Rey (2004)
California Current	33, −121	50	1984–2006	−0.62	125	Bograd et al. (2008)
California Current	33, −121	100	1984–2006	−0.74	125	Bograd et al. (2008)
California Current	33, −121	200	1984–2006	−0.99	125	Bograd et al. (2008)
California Current	33, −121	300	1984–2006	−0.81	125	Bograd et al. (2008)
California Current	33, −121	400	1984–2006	−0.30	125	Bograd et al. (2008)
California Current	33, −121	500	1984–2006	−0.15	125	Bograd et al. (2008)
Danish Coastal zone	56.58, 10.34	10	1981–2003	−0.73	1	Conley et al. (2007)
Danish Coastal zone	56.21, 11.16	20	1966–2003	−1.06	21	Conley et al. (2007)
Chesapeake Bay	38.31, −76.42	12	1985–1999	−0.08	1	Cronin and Vann (2003)
Baltic Sea	64.43, 21.86	100	1905–2000	−0.17	12	Fonselius and Valderrama (2003)
Baltic Sea	61.45, 20.04	100	1905–2000	−0.55	68	Fonselius and Valderrama (2003)
Baltic Sea	60.15, 19.11	100	1904–2000	−0.24	10	Fonselius and Valderrama (2003)
Baltic Sea	60.15, 19.11	275	1904–2000	−0.39	10	Fonselius and Valderrama (2003)
Baltic Sea	58.07, 18.32	100	1902–2000	−0.11	27	Fonselius and Valderrama (2003)
Baltic Sea	58.07, 18.32	400	1903–1999	−1.20	27	Fonselius and Valderrama (2003)
Baltic Sea	56.92, 20.16	100	1902–2000	−0.93	55	Fonselius and Valderrama (2003)
Baltic Sea	56.92, 20.16	200	1902–2000	−1.96	55	Fonselius and Valderrama (2003)
Baltic Sea	55.08, 15.91	80	1902–2000	−1.14	48	Fonselius and Valderrama (2003)
St. Lawrence Estuary	48.73,−68.59	320	1932–2003	−0.98	19	Gilbert et al. (2005)
Cabot Strait	47.33, −59.77	250	1960–2002	−0.88	30	Gilbert et al. (2005)
N Adriatic Sea	45, 13	30	1911–1984	−0.67	36	Justić et al. (1987)
East/Japan Sea	40, 135	800	1952–1999	−1.03	290	Kang et al. (2004)
East/Japan Sea	40, 135	2000	1952–1999	−0.88	290	Kang et al. (2004)
East/Japan Sea	40, 135	3000	1952–1999	−0.87	290	Kang et al. (2004)
Seto Inland Sea	34.17, 133.50	20	1978–2005	0.46	4	Kasai et al. (2007)
Black Sea	43.39, 34.06	96	1960–1995	−1.28	111	Konovalov and Murray (2001)
Black Sea	43.39, 34.06	106	1960–1995	−0.67	111	Konovalov and Murray (2001)
Black Sea	43.39, 34.06	165	1960–1995	−0.60	111	Konovalov and Murray (2001)
Black Sea	43.39, 34.06	630	1960–1995	−2.49	111	Konovalov and Murray (2001)
Black Sea	43.39, 34.06	1000	1960–1995	−5.68	111	Konovalov and Murray (2001)
Black Sea	43.39, 34.06	2000	1960–1995	−6.72	111	Konovalov and Murray (2001)

BGD
6, 9127–9160, 2009

Table 2. Continued.

Marine System	Latitude, Longitude	Depth (m)	Time period	Trend	Distance (km)	Reference
Baltic Sea	56.92, 20.16	80	1965–1994	6.45	55	Laine et al. (1997)
Baltic Sea	56.92, 20.16	150	1965–1994	−1.42	55	Laine et al. (1997)
Baltic Sea	59.02, 21.05	80	1965–1994	9.50	57	Laine et al. (1997)
Baltic Sea	59.02, 21.05	100	1965–1994	4.23	57	Laine et al. (1997)
Baltic Sea	59.02, 21.05	150	1965–1994	0.75	57	Laine et al. (1997)
Gulf of Finland	59.85, 24.83	60	1965–1994	6.19	20	Laine et al. (1997)
Gulf of Finland	59.85, 24.83	78	1965–1994	9.26	20	Laine et al. (1997)
Gulf of Finland	59.47, 22.90	70	1965–2000	4.08	31	Laine et al. (2007)
Gulf of Finland	59.85, 24.83	70	1965–2000	4.67	20	Laine et al. (2007)
Gulf of Finland	60.07, 26.35	50	1965–2000	3.21	15	Laine et al. (2007)
Yellow Sea	36.00, 122.31	39	1976–2000	−1.66	83	Lin et al. (2005)
Japan/East Sea	37.72, 134.72	500	1958–1996	0.19	182	Minami et al. (1999)
Japan/East Sea	37.72, 134.72	600	1958–1996	0.11	182	Minami et al. (1999)
Japan/East Sea	37.72, 134.72	800	1958–1996	0.40	182	Minami et al. (1999)
Japan/East Sea	37.72, 134.72	1000	1958–1996	0.19	182	Minami et al. (1999)
Japan/East Sea	37.72, 134.72	1200	1958–1996	−0.01	182	Minami et al. (1999)
Japan/East Sea	37.72, 134.72	1500	1958–1996	−0.16	182	Minami et al. (1999)
Japan/East Sea	37.72, 134.72	2000	1964–1996	−0.51	182	Minami et al. (1999)
Japan/East Sea	37.72, 134.72	2500	1965–1996	−0.53	182	Minami et al. (1999)
Japan/East Sea	40.50, 137.67	500	1965–1995	0.03	179	Minami et al. (1999)
Japan/East Sea	40.50, 137.67	600	1965–1995	−0.06	179	Minami et al. (1999)
Japan/East Sea	40.50, 137.67	800	1965–1995	0.31	179	Minami et al. (1999)
Japan/East Sea	40.50, 137.67	1000	1965–1995	0.13	179	Minami et al. (1999)
Japan/East Sea	40.50, 137.67	1200	1965–1995	0.01	179	Minami et al. (1999)
Japan/East Sea	40.50, 137.67	1500	1965–1995	−0.52	179	Minami et al. (1999)
Japan/East Sea	40.50, 137.67	2000	1965–1995	−0.64	179	Minami et al. (1999)
Japan/East Sea	40.50, 137.67	2500	1965–1995	−0.71	179	Minami et al. (1999)
Benguela Current	−26.00, 14.00	100	1994–2003	−2.48	87	Monteiro et al. (2008)
Sea of Okhotsk	50.06, 148.27	500	1960–2000	−0.54	291	Nakanowatari et al. (2007)
Oyashio	41.55, 145.36	400	1960–2000	−0.57	161	Nakanowatari et al. (2007)
Subarctic Current	45.17, 160.56	300	1963–1998	−0.23	628	Nakanowatari et al. (2007)
Gullmar Fjord	58.32, 11.55	119	1961–1996	−1.69	1	Nordberg et al. (2000)
Tianjin coastal sea	38.85, 117.75	10	1996–2006	−1.97	10	Peng et al. (2009)

Table 2. Continued.

Marine System	Latitude, Longitude	Depth (m)	Time period	Trend	Distance (km)	Reference
Scotian Shelf	43.84, −62.86	150	1961–1999	−1.06	87	Petrie and Yeats (2000)
Gulf of Maine	42.53, −67.25	150	1951–1988	0.45	138	Petrie and Yeats (2000)
Gulf of Finland	59.90, 25.04	65	1966–2000	2.09	17	Pitkänen et al. (2001)
Gulf of Finland	60.17, 26.98	55	1971–2000	−0.91	8	Pitkänen et al. (2001)
Baltic Sea (Gotland Basin)	57.32, 20.05	200	1990–2003	2.85	65	Pohl and Hennings (2005)
West coast of Sweden	58.37, 11.37	25	1962–1984	−3.51	0	Rosenberg (1990)
West coast of Sweden	58.36, 11.43	25	1963–1984	−2.49	0	Rosenberg (1990)
West coast of Sweden	58.32, 11.37	33	1964–1983	−3.25	0	Rosenberg (1990)
West coast of Sweden	58.40, 11.63	62	1968–1984	−7.23	0	Rosenberg (1990)
West coast of Sweden	58.25, 11.43	55	1952–1985	−3.66	1	Rosenberg (1990)
West coast of Sweden	58.23, 11.58	40	1951–1983	−1.30	0	Rosenberg (1990)
West coast of Sweden	58.29, 11.68	55	1951–1984	−1.41	0	Rosenberg (1990)
West coast of Sweden	58.19, 11.85	23	1952–1984	−3.97	0	Rosenberg (1990)
New York Bight	40.38, −73.74	33	1974–1985	4.69	20	Swanson and Parker (1988)
New York Bight	40.21, −73.94	22	1974–1985	2.33	5	Swanson and Parker (1988)
Louisiana Shelf	28.99, −90.07	27	1980–1995	−3.75	16	Turner et al. (2005)
Southwestern Baltic Sea	54.80, 9.96	25	1979–1993	−1.15	2	Weichart et al. (1994)
Southwestern Baltic Sea	54.59, 10.47	25	1976–1993	−6.08	19	Weichart et al. (1994)
Southwestern Baltic Sea	54.48, 9.97	25	1976–1993	−0.11	1	Weichart et al. (1994)
Southwestern Baltic Sea	54.12, 11.09	25	1976–1993	−1.50	7	Weichart et al. (1994)
Southwestern Baltic Sea	54.56, 11.35	25	1979–1993	0.66	9	Weichart et al. (1994)
Southwestern Baltic Sea	54.32, 11.57	50	1979–1993	0.59	19	Weichart et al. (1994)
Gulf of Alaska	50.00, −145.00	140	1956–2005	−0.55	912	Whitney et al. (2007)
Gulf of Alaska	50.00, −145.00	168	1956–2005	−0.79	912	Whitney et al. (2007)
Gulf of Alaska	50.00, −145.00	278	1956–2005	−0.62	912	Whitney et al. (2007)
Gulf of Alaska	50.00, −145.00	370	1956–2005	−0.27	912	Whitney et al. (2007)
Gulf of Alaska	48.66, −126.67	168	1987–2005	−1.10	71	Whitney et al. (2007)
Long Island Sound	40.51, −73.48	27	1946–2006	−1.43	10	Wilson et al. (2008)
Long Island Sound	40.47, −73.82	21	1985–2000	2.68	12	Wilson et al. (2008)
Black Sea	44.40, 38.08	70	1984–2004	−2.27	9	Yakushev et al. (2006)
Osaka Bay	34.60, 135.29	18	1972–2002	0.42	11	Yasuhara et al. (2007)
western Black Sea	42.90, 28.00	20	1961–1998	−2.14	8	Yunev et al. (2007)
western Black Sea	45.84, 31.65	20	1960–1998	−1.65	43	Yunev et al. (2007)
western Black Sea	44.80, 29.72	20	1960–1998	−1.23	10	Yunev et al. (2007)

Table 3. Oxygen trend statistics (μmol L^{-1} $year^{-1}$) from published time series in various ranges of distances from the coast. Abbreviations: C.I. = confidence interval; Std Dev = standard deviation; N = number of time series; Perc Neg = Percentage of negative trends.

Distance from coast (km)	Median	Mean	Mean 95% C.I.	Std Dev	N	Perc. Neg.	Perc. Neg. 95% C.I.	Comment
0–30	−0.98	−0.46	[−1.43, 0.52]	3.09	41	70.7	[54.5, 83.9]	+9.26 outlier (Laine et al., 1997)
30–100	−0.88	0.64	[−0.92, 2.21]	3.25	19	68.4	[43.5, 87.4]	+9.50 outlier (Laine et al., 1997)
100+	−0.54	−0.74	[−1.18, −0.30]	1.38	40	77.5	[61.5, 89.2]	
0–100+	−0.62	−0.36	[−0.88, 0.16]	2.61	100	73.0	[63.2, 81.4]	All distances combined

BGD

6, 9127–9160, 2009

BGD

6, 9127–9160, 2009

Oxygen trends in the ocean

D. Gilbert et al.

Table 4. Oxygen trend statistics (μmol L^{-1}year^{-1}) in the 0–30 km coastal band during 1976–2000. Abbreviations: C.I. = confidence interval; Std Dev = standard deviation; N [number of time series; Islands = number of time series near offshore islands; Perc Neg = Percentage of negative trends. Region abbreviations: BKS = Baltic Sea, Kattegat and Skagerack; BC = British Columbia; CalCOFI = California Cooperative Oceanic Fisheries Investigations; GSL = Gulf of St. Lawrence.

Depth (m)	Median	Mean	95% C.I.	Std Dev	N	Islands	Perc. Neg.	Regions with most time series
0	−0.22	−0.36	[−0.58, −0.15]	1.05	95	3	63.2	BKS, CalCOFI, Japan
10	−0.36	−0.60	[−0.89, −0.31]	1.42	95	3	69.5	BKS, CalCOFI, Japan
20	−0.39	−0.48	[−0.79, −0.17]	1.49	91	2	64.8	BKS, CalCOFI, Japan
50	−0.22	−0.23	[−0.55, 0.08]	1.28	64	3	57.8	BKS, CalCOFI, Japan
75	−0.01	0.37	[−0.20, 0.93]	1.80	42	3	50.0	BKS, CalCOFI, Japan
100	−0.72	−0.48	[−0.82, −0.14]	1.66	94	8	72.3	BC, BKS, CalCOFI, GSL, Japan
150	−0.26	−0.34	[−0.61, −0.07]	1.02	58	7	67.2	BC, BKS, CalCOFI, GSL, Japan
200	−0.33	−0.40	[−0.68, −0.13]	1.03	55	6	70.9	BC, BKS, CalCOFI, GSL, Japan
250	0.15	−0.07	[−0.41, 0.26]	0.94	33	5	42.4	BC, BKS, CalCOFI, GSL, Japan
300	−0.20	−0.41	[−0.80, −0.03]	0.93	25	2	60.0	CalCOFI, GSL, Japan
0 to 300	−0.28	−0.35	[−0.47, −0.24]	1.22	424	34	64.2	

Table 5. Oxygen trend statistics (μmol L^{-1}year^{-1}) in the transition band, between 30 and 100 km from the shoreline, during 1976–2000. Abbreviations: C.I. = confidence interval; Std Dev = standard deviation; N = number of time series; Perc Neg = Percentage of negative trends. Region abbreviations: BKS = Baltic Sea, Kattegat and Skagerack; CalCOFI = California Cooperative Oceanic Fisheries Investigations; ECS = East China Sea; EJS = East/Japan Sea, GSL = Gulf of St. Lawrence.

Depth (m)	Median	Mean	95% C.I.	Std Dev	N	Perc. Neg.	Regions with most time series
0	−0.08	−0.22	[−0.39, −0.05]	0.82	89	57.3	BKS, CalCOFI, Japan
10	−0.05	−0.19	[−0.35, −0.03]	0.76	91	59.3	BKS, CalCOFI, ECS, EJS, Japan
20	−0.17	−0.41	[−0.72, −0.11]	1.39	82	58.5	BKS, CalCOFI, ECS, EJS, Japan
50	−0.30	−0.32	[−0.63, −0.01]	1.44	85	62.4	BKS, CalCOFI, ECS, EJS, Japan
75	0.25	0.42	[0.02, 0.82]	1.75	76	38.2	BKS, CalCOFI, ECS, EJS, Japan
100	−0.22	−0.17	[−0.39, 0.05]	1.21	120	60.0	BKS, CalCOFI, ECS, EJS, GSL, Japan
150	−0.05	−0.02	[−0.21, 0.17]	0.99	103	50.5	BKS, CalCOFI, ECS, EJS, GSL, Japan
200	−0.15	−0.21	[−0.40, −0.02]	0.96	100	60.0	CalCOFI, ECS, EJS, GSL, Japan
250	−0.16	−0.22	[−0.44, −0.01]	0.89	69	58.0	CalCOFI, EJS, GSL, Japan
300	−0.13	−0.19	[−0.48, 0.10]	1.18	66	54.5	CalCOFI, EJS, GSL, Japan
0 to 300	−0.15	−0.19	[−0.27, −0.10]	1.09	632	57.6	

Table 6. Oxygen trend statistics (μmol L^{-1}year^{-1}) in the open ocean, more than 100 km from the shoreline, during 1976–2000. Abbreviations: C.I. = confidence interval; Std Dev = standard deviation; N = number of time series; Perc Neg = Percentage of negative trends. Region abbreviations: CalCOFI = California Cooperative Oceanic Fisheries Investigations; ECS = East China Sea; EJS = East/Japan Sea, NAtl = North Atlantic; WPac = West Pacific.

Depth (m)	Median	Mean	95% C.I.	Std Dev	N	Perc. Neg.	Regions with most time series
0	−0.03	−0.05	[−0.12, 0.03]	0.55	201	53.7	CalCOFI, ECS, EJS, NAtl, WPac
10	−0.08	−0.19	[−0.29, −0.10]	0.61	161	60.2	CalCOFI, ECS, EJS, NAtl, WPac
20	−0.30	−0.44	[−0.67, −0.21]	1.30	125	65.6	CalCOFI, ECS, EJS, NAtl, WPac
50	−0.11	−0.20	[−0.35, −0.05]	1.03	190	58.4	CalCOFI, ECS, EJS, Line P, NAtl, WPac
75	−0.05	−0.09	[−0.25, 0.06]	0.98	162	52.5	CalCOFI, ECS, EJS, NAtl, WPac
100	0.03	−0.08	[−0.21, 0.05]	1.39	426	47.9	CalCOFI, ECS, EJS, Line P, NAtl, WPac
150	0.07	0.01	[−0.13, 0.14]	1.38	420	46.0	CalCOFI, ECS, EJS, LineP, NAtl, WPac
200	0.04	−0.10	[−0.24, 0.05]	1.47	412	47.1	CalCOFI, EJS, Line P, NAtl, WPac
250	0.09	−0.05	[−0.22, 0.13]	1.66	349	44.7	CalCOFI, EJS, Line P, NAtl, WPac
300	−0.04	−0.23	[−0.40, −0.06]	1.58	332	53.3	CalCOFI, EJS, Line P, NAtl, WPac
0 to 300	0.02	−0.09	[−0.15, −0.03]	1.40	2330	49.1	

BGD
6, 9127–9160, 2009

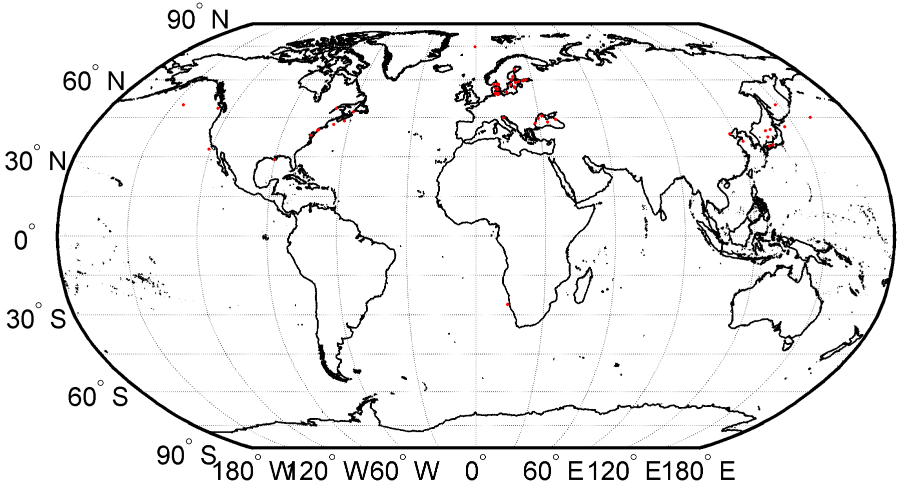

Fig. 1. Station locations (red dots) of digitized oxygen concentration time series from refereed journal publications.

BGD
6, 9127–9160, 2009

Oxygen trends in the ocean

D. Gilbert et al.

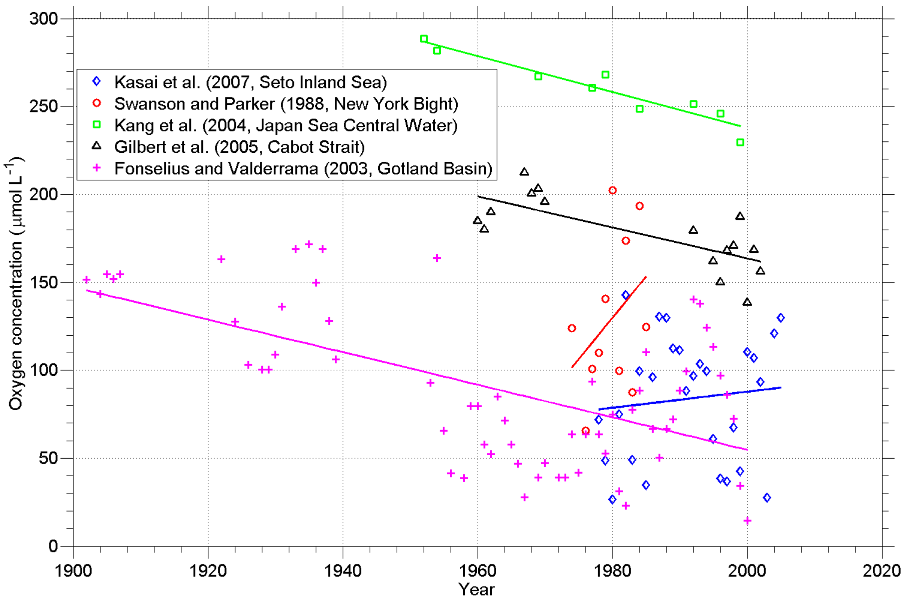

Fig. 2. Examples of digitized oxygen time series from refereed journal papers, and our fitted linear trends. The Gotland Basin time series is from 100 m depth.

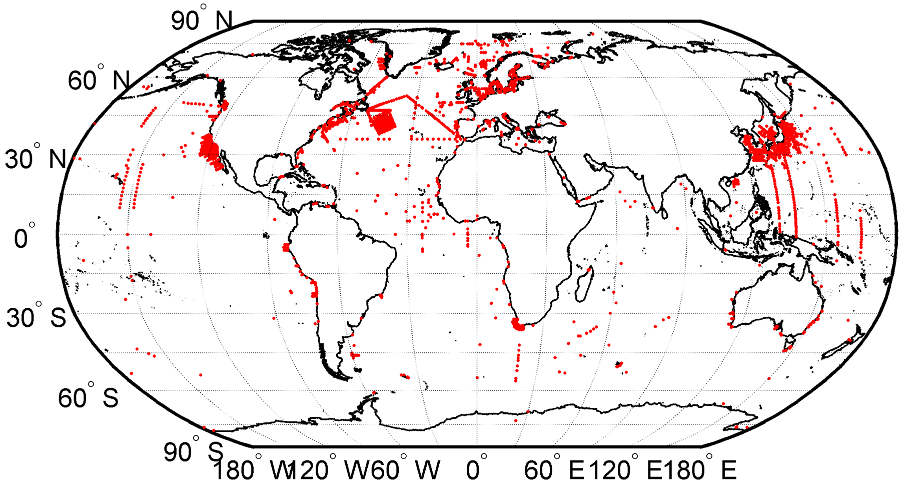

Fig. 3. Station locations (red dots) of oxygen concentration time series constructed from a global oxygen database.

BGD
6, 9127–9160, 2009

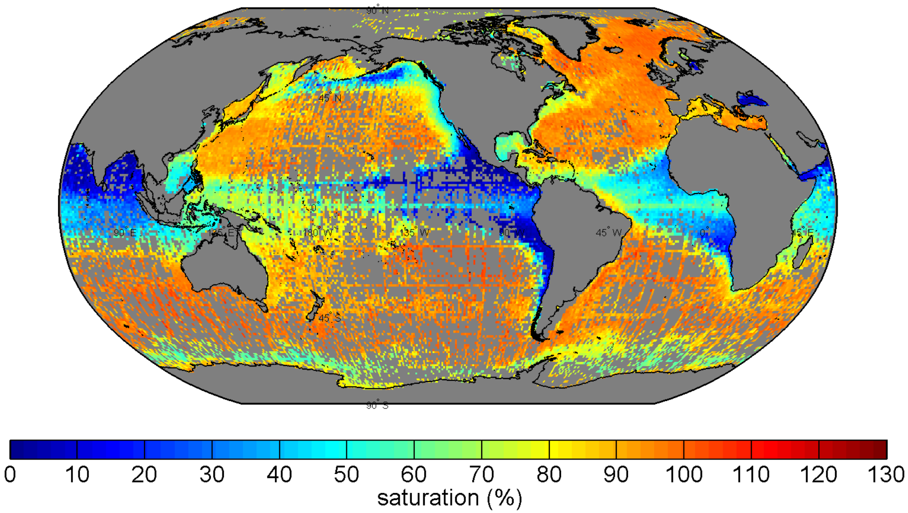

Fig. 4. Oxygen saturation percentage at 150 m depth, averaged over 1° of latitude × 1° of longitude polygons, based on the global oxygen database used in this study. No interpolation was performed, and the grey areas indicate absence of data.

BGD
6, 9127–9160, 2009

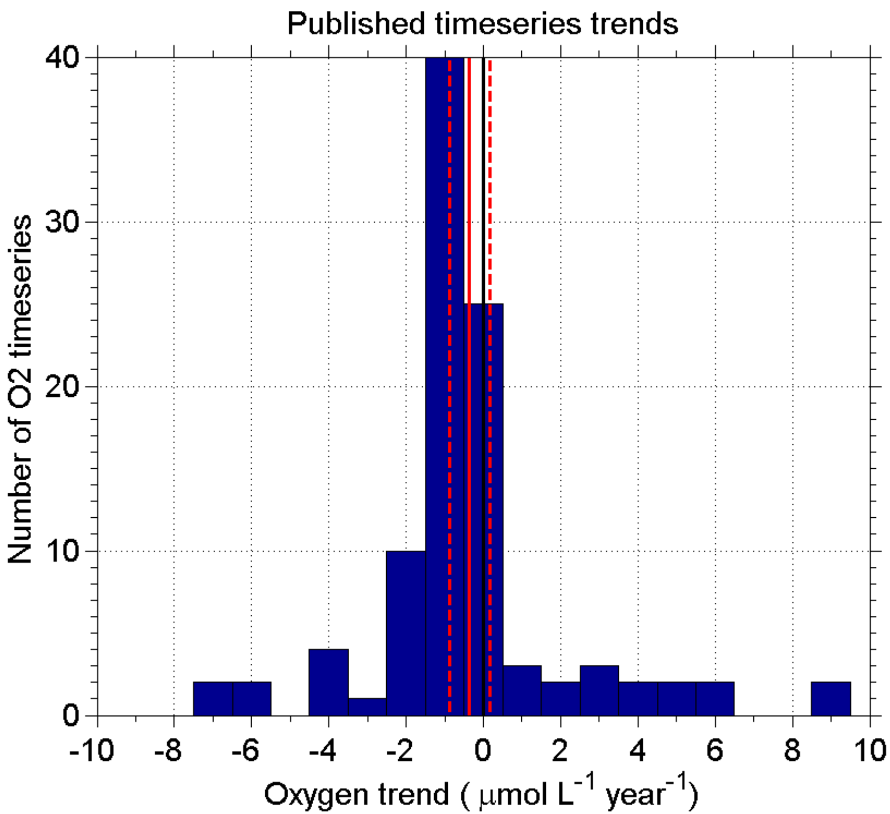

Fig. 5. Histogram of oxygen concentration trends calculated from oxygen time series published in refereed journals (Table 2).

BGD
6, 9127–9160, 2009

Oxygen trends in the ocean

D. Gilbert et al.

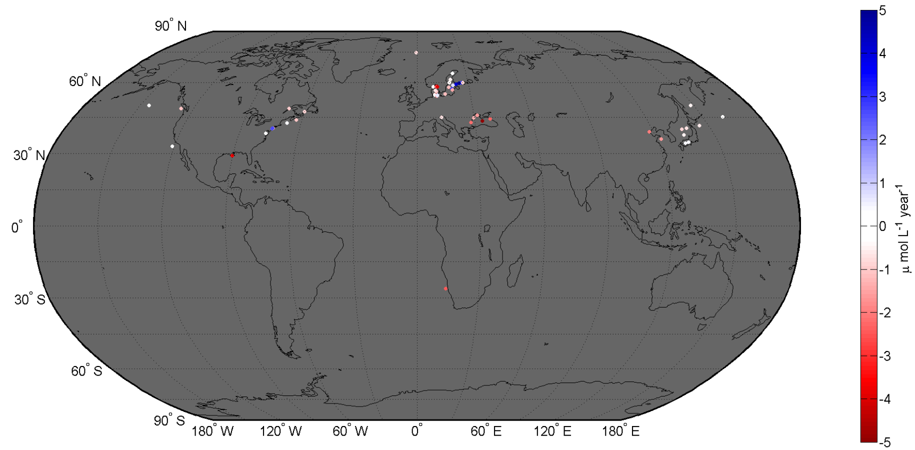

Fig. 6. Map of oxygen trends from refereed journal publications (Table 2).

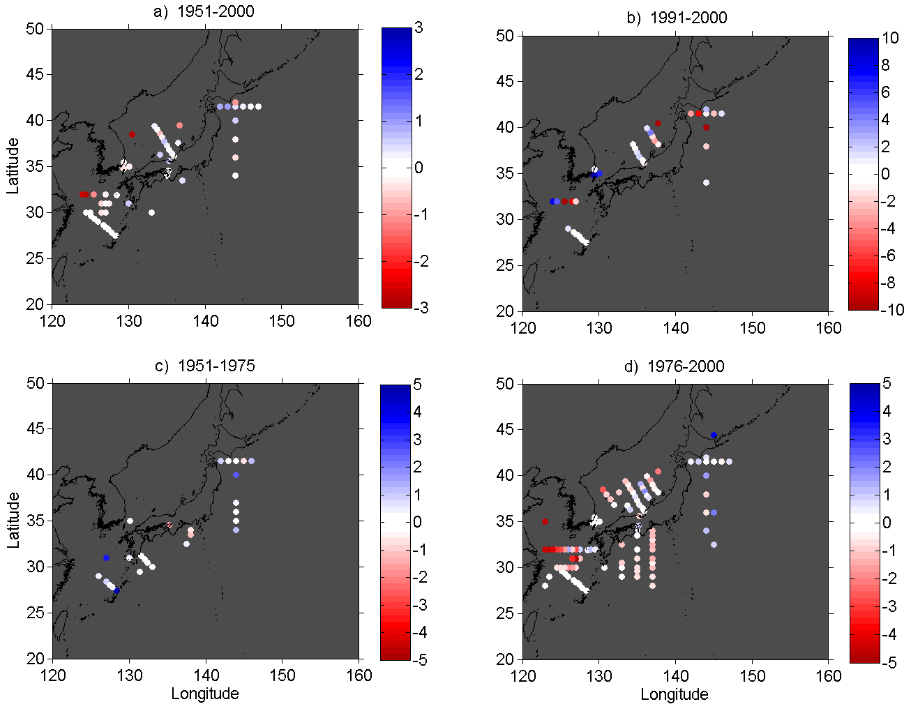

Fig. 7. Oxygen concentration trends (μmol L^{-1}yr^{-1}) computed from a global oxygen database at 20 m depth around Japan for **(a)** 1951–2000, **(b)** 1991–2000, **(c)** 1951–1975, **(d)** 1976–2000.

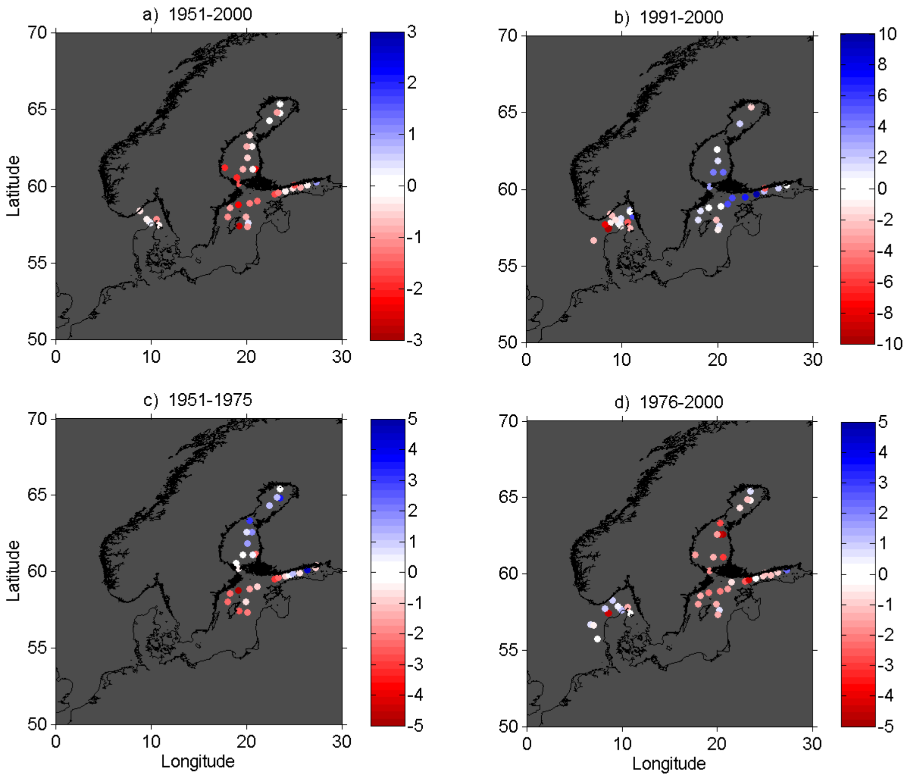

Fig. 8. Oxygen concentration trends (μmol $L^{-1}yr^{-1}$) computed from a global oxygen database at 20 m depth around Europe for **(a)** 1951–2000, **(b)** 1991–2000, **(c)** 1951–1975, **(d)** 1976–2000.